NANO LETTERS

Letter

pubs.acs.org/NanoLett

Ionic Conductivity Enhancement of Polymer Electrolytes with Ceramic Nanowire Fillers

Wei Liu,[†] Nian Liu,[†] Jie Sun,[†] Po-Chun Hsu,[†] Yuzhang Li,[†] Hyun-Wook Lee,[†] and Yi Cui*[,†,‡]

[†]Department of Materials Science and Engineering, Stanford University, Stanford, California 94305, United States

[‡]Stanford Institute for Materials and Energy Sciences, SLAC National Accelerator Laboratory, 2575 Sand Hill Road, Menlo Park, California 94025, United States

Supporting Information

ABSTRACT: Solid-state electrolytes provide substantial improvements to safety and electrochemical stability in lithium-ion batteries when compared with conventional liquid electrolytes, which makes them a promising alternative technology for next-generation high-energy batteries. Currently, the low mobility of lithium ions in solid electrolytes limits their practical application. The ongoing research over the past few decades on dispersing of ceramic nanoparticles into polymer matrix has been proved effective to enhance ionic conductivity although it is challenging to form the efficiency networks of ionic conduction with nanoparticles. In this work, we first report that ceramic nanowire fillers can facilitate formation of such ionic conduction networks in polymer-based solid electrolyte to enhance its ionic conductivity by three orders of magnitude. Polyacrylonitrile-$LiClO_4$ incorporated with 15 wt % $Li_{0.33}La_{0.557}TiO_3$ nanowire composite electrolyte exhibits an unprecedented ionic conductivity of 2.4×10^{-4} S cm^{-1} at room temperature, which is attributed to the fast ion transport on the surfaces of ceramic nanowires acting as conductive network in the polymer matrix. In addition, the ceramic-nanowire filled composite polymer electrolyte shows an enlarged electrochemical stability window in comparison to the one without fillers. The discovery in the present work paves the way for the design of solid ion electrolytes with superior performance.

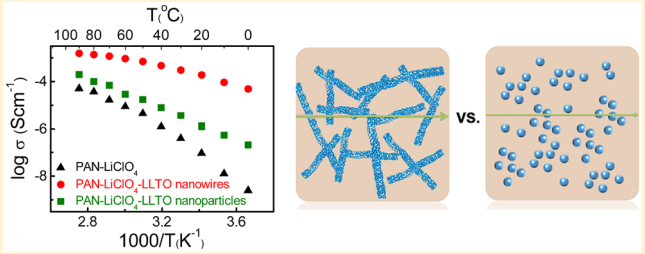

KEYWORDS: *Solid composite electrolyte, nanowires, polyacrylonitrile, ionic conductivity*

Lithium-ion batteries have been intensively studied in order to meet the ever-growing demands of technologies ranging from portable devices and electric vehicles to grid-scale energy storages.[1−6] Safety is one of the most urgent concerns associated with further advances in next-generation high-energy batteries, making solid electrolytes among the most promising candidates to replace flammable and potentially dangerous liquid electrolytes. In addition to the inorganic lithium ion electrolytes,[7−10] much attention has been devoted to blend various kinds of lithium salts with solid polymer electrolytes (SPE), such as polyacrylonitrile (PAN) and related polymer-based (e.g., poly(ethylene oxide), poly(vinylidene fluoride), poly(methyl methacrylate)) solid electrolytes.[4−6,11,12] However, because of their low ionic conductivities at room temperature (which is below their glass transition temperatures) and poor electrochemical stability, solid polymer electrolytes have not been widely used in commercial lithium-ion batteries. To address these concerns, previous approaches including cross-linking, using diblock copolymer, or adding plasticizers have been investigated. Unfortunately, these modifications diminish performance by loss of ionic conductivity and compatibility with lithium electrodes, and by deterioration of mechanical properties and flame resistivity.[3,12,13] In contrast, dispersing ceramic particles in polymer matrix increases ionic conductivity effectively, meanwhile improving electrochemical stability and mechanical strength. The addition of these ceramic particle fillers is believed to hinder the polymer crystallization or to contribute highly conductive interface layers between polymer and ceramic.[14−18] The ceramic fillers are generally divided into two categories: inactive fillers that are not involved in lithium ion conduction process (e.g., Al_2O_3[14] and SiO_2[15]) and active ones that participate in lithium ion transport (e.g., Li_3N[16] and $Li_{1.3}Al_{0.3}Ti_{1.7}(PO_4)_3$[17]).

Nanoscale ceramic fillers have large specific surface area and can enhance the ionic conductivity drastically.[19] Most research has emphasized ceramic nanoparticles,[15−18] whereas little attention has been given to one-dimensional ceramic fillers. Here we explore nanowire fillers and demonstrate significant improvement of ionic conductivity and electrochemical stability. Compared with nanoparticle fillers, in which Li^+ must cross a lot of particle−particle junctions, nanowire fillers with high aspect ratio embedded in polymer electrolyte can create continuous ionic transport pathways to much longer distances, reducing the junction cross significantly. We fabricated $Li_{0.33}La_{0.557}TiO_3$ (LLTO) nanowires via electrospinning for the first time, and dispersed them into PAN-

Received: February 12, 2015
Revised: March 7, 2015
Published: March 17, 2015

DOI: 10.1021/acs.nanolett.5b00600
Nano Lett. 2015, 15, 2740−2745

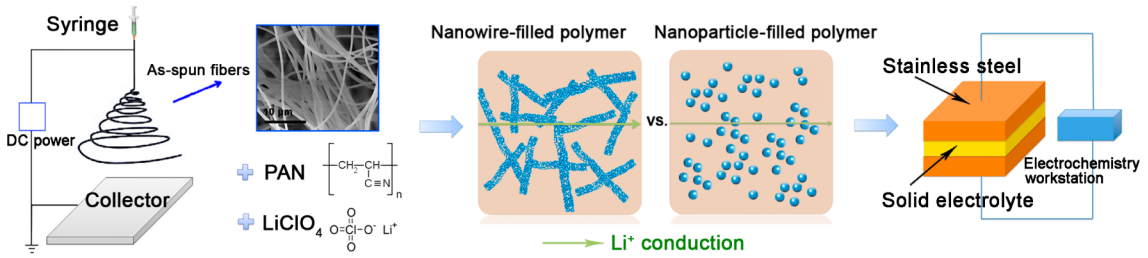

Figure 1. Schematic illustration for the synthesis of ceramic nanowire-filled polymer-based composite electrolytes, together with the comparison of possible lithium-ion conduction pathway in nanowire-filled and nanoparticle-filled composite electrolytes, and illustration of the electrode configuration for the AC impedance spectroscope measurement.

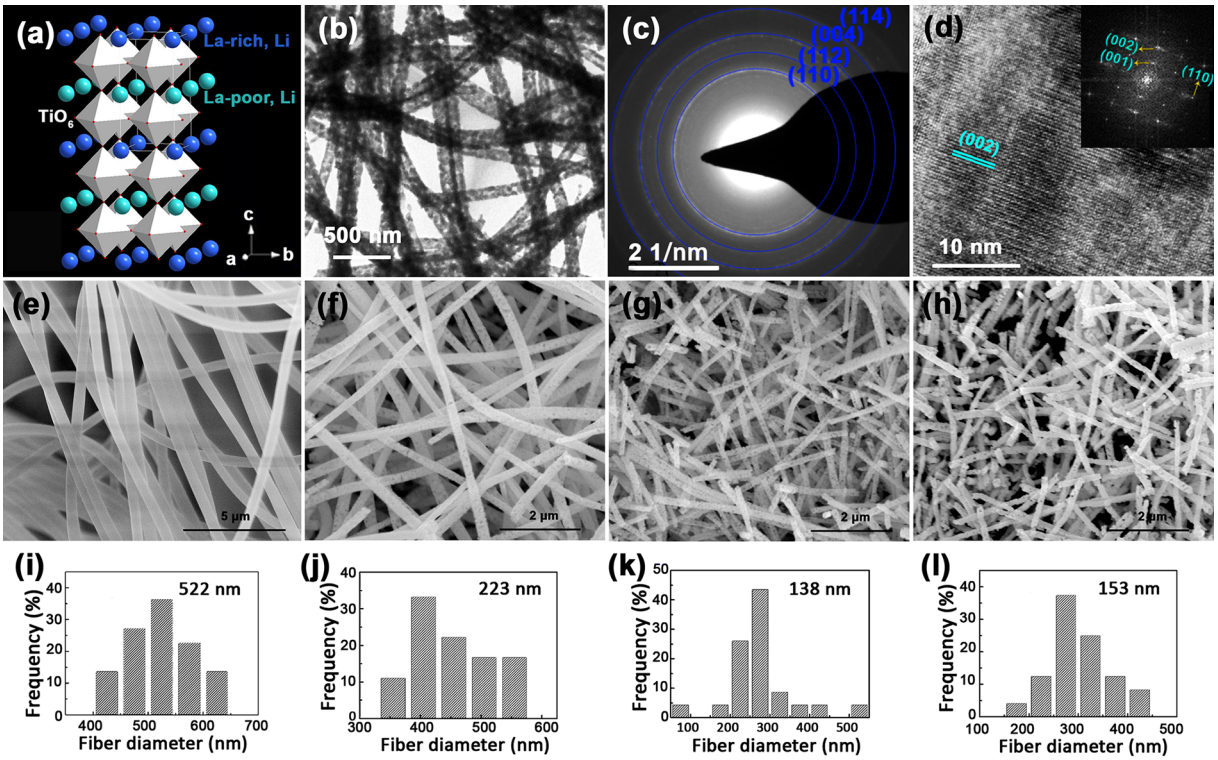

Figure 2. Morphologies of LLTO nanowires. (a) Perspective view of LLTO. (b) TEM image of LLTO nanowires, with (c) corresponding SAED pattern. (d) HRTEM image of an individual LLTO nanowire, with inset FFT pattern. (e) SEM image of as-spun fibers. SEM images of LLTO nanowires calcined at (f) 700 °C, (g) 800 °C, and (h) 900 °C, with corresponding diameter distributions and average diameters (i–l).

$LiClO_4$ polymer without any other additive to prepare a novel solid composite polymer electrolyte. As a representative solid lithium-ion conductor, $Li_{3x}La_{2/3-x}\square_{1/3-2x}TiO_3$ ($0<x<0.167$) is A-site deficient of the perovskite (ABO_3) and has been reported to exhibit a high bulk ionic conductivity of 1.0×10^{-3} S cm^{-1} ($x \approx 0.11$) at room temperature.[20−23] The microstructure and conductivity of ceramic nanowire-filled composite polymer-based electrolytes were systematically investigated.

As shown in Figure 1, the schematic illustration indicates the procedure to synthesize LLTO nanowire-filled PAN-$LiClO_4$ composite electrolytes. LLTO nanowires were prepared by electrospinning of polyvinylpyrrolidone polymer fiber containing the relevant salts and then calcined at the temperature range of 600−900 °C in air for 2 h (for details, see Experimental Methods in Supporting Information). Differential thermal analysis (DTA) curves of as-synthesized polymer fibers (Figure S1) show that above 700 °C there was no obvious thermal change, indicating the complete formation of LLTO, which is consistent with the thermogravimetric (TG) result. Subsequently, 5−20 wt % (total weight of PAN and $LiClO_4$) of LLTO nanowires were added in the dimethylformamide (DMF) solution containing PAN and $LiClO_4$. The mixture was mechanically stirred at 80 °C for 5 h and then cast with a doctor blade on to a glass plate. Finally, the composite polymer electrolyte was dried in high vacuum overnight to completely remove the DMF solvent. The possible lithium ion conduction pathway in nanowire-filled and nanoparticle-filled composite polymer electrolytes is also illustrated in Figure 1, respectively.

The crystalline phase evolution of LLTO nanowires calcined at variable temperatures from 600 to 900 °C has been examined by X-ray diffraction (XRD) measurements. Figure S2 displays the XRD patterns of LLTO nanowires, which indicates that all peaks could be indexed to a primarily perovskite structure with the tetragonal *P*4/*mmm* space group. Figure 2a depicts the crystal structure consisting of alternate La-rich and La-poor layers. Morphologies of the nanowires were examined by transmission electron microscopy (TEM) and scanning electron microscopy (SEM), as shown in Figure 2b−h.

DOI: 10.1021/acs.nanolett.5b00600
Nano Lett. 2015, 15, 2740−2745

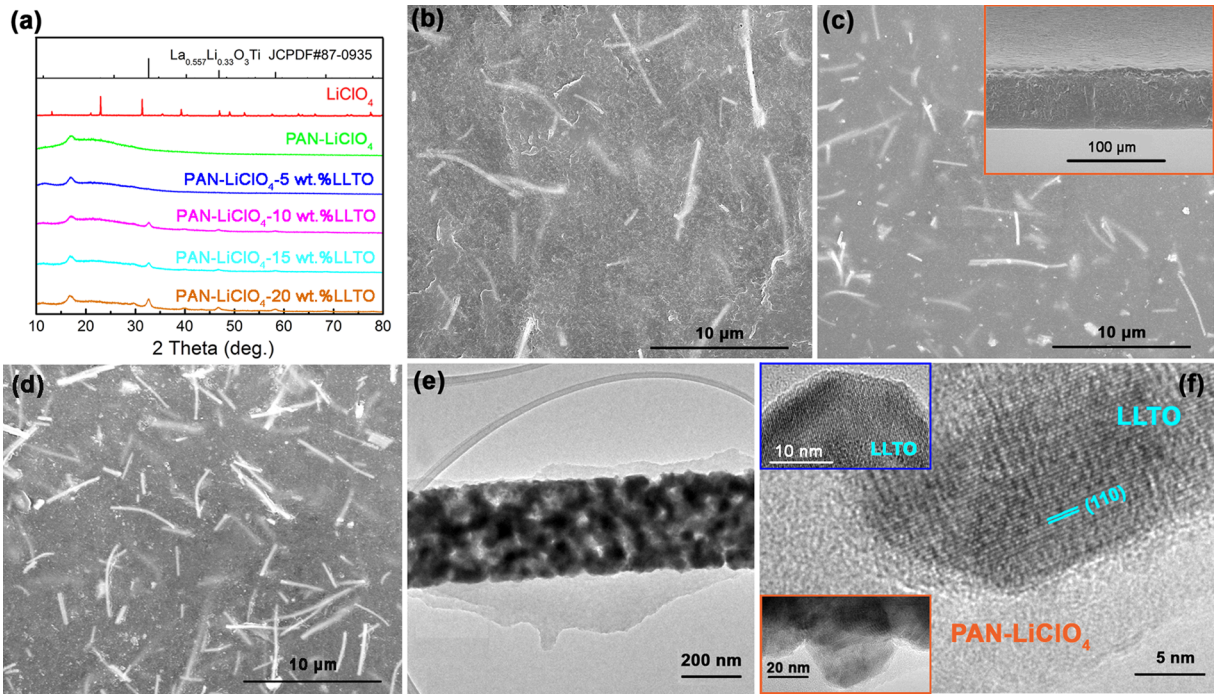

Figure 3. Phase structure and morphology of the composite electrolytes with various contents of LLTO nanowires. (a) XRD patterns of the composite electrolytes with various LLTO concentrations of 5−20 wt %. SEM images for the composite electrolytes with (b) 10 wt %, (c) 15 wt %, and (d) 20 wt % nanowire fillers. (e) TEM image and (f) HRTEM image of the composite electrolyte with 15 wt % nanowires, respectively. In panel f, the upper inset is the HRTEM image for LLTO nanowire, and the bottom one illustrates the individual grain of the nanowires embedded in PAN matrix.

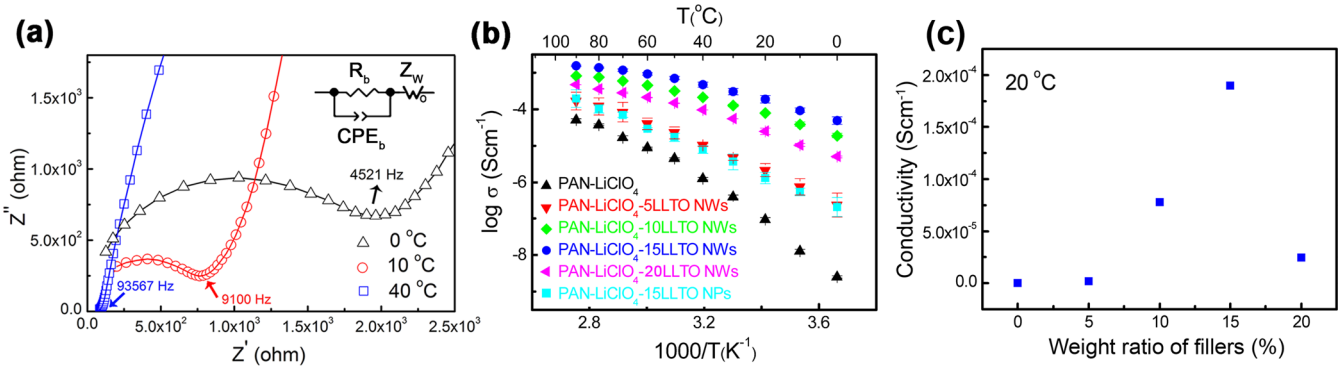

Figure 4. Electrical properties of solid composite polymer electrolytes. (a) Experimental and fitting impedance spectra for the composite electrolyte with 15 wt % LLTO nanowires at different measuring temperatures, and the equivalent circuit. In the equivalent circuit, R_b is the bulk resistance of the polymer electrolytes and CPE_b is the constant phase element to fit bulk capacitance. The straight line in the lower frequencies is due to an ion diffusion-limited process contributing to an impedance response (Warburg impedance Z_w). (b) Arrhenius plots of the composite electrolytes with various LLTO nanowire concentrations, together with the date for LLTO nanoparticle-filled PAN-$LiClO_4$ electrolyte. (c) Conductivity of the composite polymer electrolyte as a function of the weight ratio of nanowire fillers.

Identical morphological features of individual LLTO nanowires calcined at 800 °C with large aspect ratios can be observed in Figure 2b. The corresponding selected area electron diffraction (SAED) pattern in Figure 2c shows a polycrystalline structure that can correspond to a tetragonal cell, which is in agreement with XRD pattern results. Figure 2d shows the high resolution TEM (HRTEM) image of individual LLTO grain indicating excellent crystallinity within each grain. Together with the fast-Fourier transform (FFT) pattern along [010] zone axis shown in the inset, this confirms the tetragonal perovskite structure. SEM image in Figure 2e shows that as-spun fibers have smooth surfaces with an average diameter of 520 nm. After thermal treatment at 700 °C for 2 h, the diameter of the nanowires decreases considerably to 220 nm (Figure 2f) and further decreases to 140 nm if using a calcination temperature of 800 °C (Figure 2g). The diameter of LLTO nanowires increases when improving the calcination temperature to 900 °C (Figure 2h), which is due to the growth of grains, resulting in coarse surfaces as well. Providing the largest specific surface area, LLTO nanowires calcined at 800 °C were selected as the fillers dispersed into PAN matrix for further study.

XRD patterns taken at room temperature for PAN-$LiClO_4$ and the composite electrolytes are given in Figure 3a. A peak around 17° is observed that can be indexed into the characteristic diffraction peak of PAN. It also can be seen that, due to the complexation between $LiClO_4$ and PAN, the

DOI: 10.1021/acs.nanolett.5b00600
Nano Lett. 2015, 15, 2740−2745

diffraction peaks of $LiClO_4$ are absent in PAN-based electrolyte, which indicates no salt particles in the composite electrolyte. Figure 3a also indicates that dispersing 5−20 wt % LLTO nanowires into PAN has no obvious influence on the crystallinity of PAN, as the relative intensity of the peak corresponding to PAN is almost unchanged. The microstructures of the composite electrolytes with various contents of 10−20 wt % nanowires are shown in Figure 3b−d, which demonstrates a random distribution of LLTO nanowires free of aggregates in the PAN matrix. TEM images of the composite electrolyte with 15 wt % nanowires in Figure 3e,f clearly show that LLTO nanowires are fully embedded inside PAN. For preparation of the TEM specimen, the DMF solution containing LLTO nanowires, $LiClO_4$, and 10 wt % PAN was further diluted by DMF and then loaded on lacey TEM grids.

The ionic conductivities of solid electrolytes were investigated via AC impedance spectroscopy measurements with two stainless steel blocking electrodes. With well-fitted spectra, typical AC impedance spectra for the composite electrolyte measured at various temperatures are given in Figure 4a. One can see a well-defined semicircle at high and intermediate frequencies that is ascribed to the parallel combination of bulk resistance and bulk capacitance, which is as a result of the migration of ions and the immobile polymer chains, respectively. The spike at low frequencies corresponds to the double layer capacitance formed at the interface between electrode and electrolyte.[14,24−26] The ionic conductivity σ data for electrolytes can be converted from a resistance R data measured at different temperatures, as shown in the following equation:

$$\sigma = \frac{1}{R}\frac{L}{S} \tag{1}$$

where L is the membrane thickness and S is the effective electrode area. The temperature dependence of the ionic conductivity for solid composite electrolytes over the range of LLTO nanowire calcined at 800 °C with contents from 5 to 20 wt % is shown in Figure 4b. For comparison, the ionic conductivity of LLTO nanoparticle-filled (15 wt %) PAN-$LiClO_4$ electrolyte is also shown in this figure. Compared to the solid polymer electrolyte without fillers (Figure 4b), an appreciable enhancement of conductivity could be detected throughout all filler blending contents. The composite electrolyte containing 15 wt % LLTO nanowires displays the highest conductivity of 2.4×10^{-4} S cm^{-1} at room temperature, which is about three orders of magnitude higher than that of PAN-$LiClO_4$ without fillers (2.1×10^{-7} S cm^{-1}). In addition, as shown in Figure 4c, the conductivity of the composite polymer electrolyte has a sharp turn at ∼10% and reaches the maximum at 15%, then drops rapidly at 20%, showing a percolation behavior.[27] However, the conductivity reduction at high weight percentage (20%) in our case might result from the aggregation of the nanowires taken place at high weight ratio loading (Figure 3d). Dispersion of more LLTO nanowires results in more disparity of the lithium distribution, easier aggregation of nanowires, and reduced miscibility between PAN and LLTO, eventually leading to phase separation and loss of ionic conductivity. Besides the superior conductivity, the composite polymer electrolytes also demonstrate better electrochemical stability than PAN-$LiClO_4$ electrolyte (Figure S3).

Over the years, one to two orders of magnitude enhancement of conductivity has been achieved in previous reports by adding ceramic nanoparticles,[28−30] whereas in the present work more than three orders of magnitude improvement was realized by blending Li-conducting ceramic nanowires with PAN-$LiClO_4$. Some previous papers[11,28,31] reported that the enhancement of conductivity by the addition of ceramic fillers is due to the reduction of polymer crystallinity and more flexible local chains in the amorphous phase. In this study, we confirm that filling LLTO nanowires could not influence the crystallinity of PAN. The degree of crystallization of PAN is known to affect its dehydrogenation temperature. Herein, the thermal behaviors of PAN-$LiClO_4$ and the one filled with 15 wt % LLTO nanowire are characterized using TG shown in the Figure S4, as observed in which the rapid weight loss around 351 °C is mainly due to the dehydrogenation of PAN. By filling 15 wt % LLTO nanowires, the dehydrogenation temperature of PAN reduces slightly to 344 °C, which indicates that the dehydrogenation is not promoted noticeably by the filling of LLTO nanowires. As for a higher degree of crystallization, a higher dehydrogenation temperature is needed, so the addition of LLTO nanowires into PAN results in little deterioration of PAN crystallinity. As a consequence, reduction of polymer crystallinity is not a predominate reason for the conductivity improvement of the composite electrolyte.

In general, the relationship between ionic conductivity and temperature for the polymer electrolyte follows the classical Arrhenius relationship:

$$\sigma(T) = A \exp\left(-\frac{E_a}{RT}\right) \tag{2}$$

where T is the absolute temperature, E_a the activation energy, and A is a pre-exponential factor.[32,33] For PAN-based polymer electrolytes, lithium ions diffuse in the amorphous phase with the assistance of chain segments of PAN. This can be attributed to an interaction between lithium salt and C≡N of PAN where lithium ions move toward the electron rich group of PAN. Figure 4b also demonstrates that, by introducing ceramic-nanowire fillers into PAN-$LiClO_4$ electrolyte, the slope of the temperature dependence of ionic conductivity decreases, which indicates a lower activation energy (see Table S1) and accordingly implies a diverse conduction mechanism rather than the ion random walking through amorphous PAN for the composite electrolyte.[30,32−35]

Another conduction mechanism is established by lithium-ion hopping in a sequential manner on the skin areas of ceramic fillers, which is achieved by replacing a nearby vacancy.[34−36] It is well-known that the mobility and concentration of free Li^+ play the most important role in the ionic conductivity of solid electrolytes, which are affected by the interaction between lithium ions and polymer. Wieczorek et al.[37] applied the Lewis acid−base theory to explain the conductivity enhancement for the case of inorganic nanoparticle-filled polymer electrolyte. It is proposed that a stronger affinity can be expected between ClO_4^- and acidic groups on the surface of nano-oxides, which helps to separate the $Li^+ClO_4^-$ ion pairs and results in an increase in concentration of free Li^+ ions.[38] In addition, it is well-known that LLTO is A-site deficient of the perovskite-type lithium ion conductor. The surface region is enriched with vacancies that allow Li-ion to hop from one vacancy to the next one. That is, the surface area of LLTO nanowires supplies a fast pathway for Li^+ diffusion, which results in increased ion mobility. Compared with PAN-based polymer electrolyte, the mechanism of lithium ions replacing the nearby vacancies in LLTO nanowire-filled composite electrolyte could result in a

DOI: 10.1021/acs.nanolett.5b00600
Nano Lett. 2015, 15, 2740−2745

lower activation energy, which is pinpointed by the slopes of plots in Figure 4b. Therefore, both the concentration and mobility of Li^+ are improved on the nanowire surfaces in the composite electrolyte.

Furthermore, the ceramic nanowires of high aspect ratio filled in polymer matrix supply a 3D ion-conducting network pathway, providing long-range Li^+ transfer channels, which is beyond the ability of nanoparticles that have an isolated distribution in polymer matrix. Figure 1 illustrates the possible lithium-ion conduction pathways in nanowire-filled and nanoparticle-filled composite polymer electrolytes, respectively. As shown in Figure 4b, the conductivity enhancement for the composite electrolyte by filling LLTO nanoparticles (see Figure S5 for the microstructure) is one order of magnitude greater, while filling LLTO nanowires offers three orders of magnitude improvement, with the same percentage (15 wt %) of ceramic fillers and similar grain size (~50 nm diameter). Additionally, nanoparticle aggregation might also contribute to the lower ionic conductivity since the aggregation would further reduce probability of forming the ionic percolation. Therefore, anomalous conductivity enhancement in nanowire-filled PAN-$LiClO_4$ composite electrolyte is achieved mainly due to the fast conductive networks formed by nanowire morphology of Li-conducting fillers. The detailed mechanism for the enhancement of conductivity in the composite electrolyte, however, needs further investigation.

In summary, LLTO nanowires have been successfully prepared by electrospinning for the first time. The results show that the ionic conductivity of LLTO nanowire-filled PAN-based solid composite polymer electrolyte is higher in comparison to the state-of-the-art composite electrolyte with ceramic nanoparticles at the same blending level. A superior conductivity of 2.4×10^{-4} S cm^{-1} at room temperature for the composite electrolyte with 15 wt % LLTO nanowires is achieved. Our work opens the door for novel developments of one-dimensional Li^+-conducting ceramic materials in solid electrolytes for lithium-ion batteries.

■ ASSOCIATED CONTENT

Ⓢ Supporting Information

Detailed description of the experimental procedures, DTA/TG and XRD characterization of LLTO nanowires, TG curves of solid electrolytes, SEM images of LLTO nanopowder and composite electrolyte filled with LLTO nanoparticles, and supplementary electrochemical data. This material is available free of charge via the Internet at http://pubs.acs.org.

■ AUTHOR INFORMATION

Corresponding Author

*E-mail: yicui@stanford.edu.

Author Contributions

W.L. and Y.C. conceived the experiment and carried out data analysis. W.L. performed materials fabrication and characterization. N.L., J.S., P.H., and H.L. assisted in experimental work. W.L., N.L., Y.L., and Y.C. wrote the paper. All the authors discussed the results and commented on the manuscript.

Notes

The authors declare no competing financial interest.

■ ACKNOWLEDGMENTS

This work was supported by the Samsung Global Research Partnership Program.

■ REFERENCES

(1) Goodenough, J. B.; Kim, Y. *J. Power Sources* **2011**, *196*, 6688–6694.
(2) Wu, H.; Cui, Y. *Nano Today* **2012**, *7*, 414–429.
(3) Bouchet, R.; Maria, S.; Meziane, R.; Aboulaich, A.; Lienafa, L.; Bonnet, J. P.; Trang, N. T. P.; Bertin, D.; Gigmes, D.; Devaux, D. *Nat. Mater.* **2013**, *12*, 452–457.
(4) Denoyel, R.; Armand, M.; Fergus, J. W. *J. Power Sources* **2010**, *195*, 4554–4569.
(5) Quartarone, E.; Mustarelli, P. *Chem. Soc. Rev.* **2011**, *40*, 2525–2540.
(6) Smith, D. M.; Dong, B.; Marron, R. W.; Birnkrant, M. J.; Elabd, Y. A.; Natarajan, L. V.; Tondiglia, V. P.; Bunning, T. J.; Li, C. Y. *Nano Lett.* **2011**, *12*, 310–314.
(7) Takada, K. *Acta Mater.* **2013**, *61*, 759–770.
(8) Kamaya, N.; Homma, K.; Yamakawa, Y.; Hirayama, M.; Kanno, R.; Yonemura, M.; Mitsui, A. *Nat. Mater.* **2011**, *10*, 682–686.
(9) Seino, Y.; Ota, T. T. K.; Hayashi, A.; Tatsumisago, M. *Energy Environ. Sci.* **2014**, *7*, 627–631.
(10) Liu, Z.; Fu, W.; Payzant, E. A.; Yu, X.; Wu, Z.; Dudney, N. J.; Liang. *J. Am. Chem. Soc.* **2013**, *135*, 975–978.
(11) Croce, F.; Appetecchi, G. B.; Persi, L.; Scrosati, B. *Nature* **1998**, *394*, 456–458.
(12) Min, H. S.; Ko, J. M.; Kim, D. W. *J. Power Sources* **2003**, *119–121*, 469–472.
(13) Stephan, M. *Eur. Polym. J.* **2006**, *42*, 21–42.
(14) Qian, X.; Gu, N.; Cheng, Z.; Yang, X.; Wang, E.; Dong, S. *Electrochim. Acta* **2001**, *46*, 1829–1836.
(15) Kim, J. W.; Ji, K. S.; Lee, J. P.; Park, J. W. *J. Power Sources* **2003**, *119–121*, 415–421.
(16) Stephan, A. M.; K, S. *Polymer* **2006**, *47*, 5952–5964.
(17) Wang, Y. J.; Pan, Yi; Kim, D. *J. Power Sources* **2006**, *159*, 690–701.
(18) Balazs, A. C.; Emrick, T.; Russell, T. P. *Science* **2006**, *314*, 1107–1110.
(19) Kumar, B.; Scanlon, L. G. *J. Power Sources* **1994**, *52*, 261–268.
(20) Inaguma, Y.; C. Itoh, L. M.; Nakamura, T.; Uchida, T.; Ikuta, H.; Wakihara, M. *Solid State Commun.* **1993**, *86*, 689–693.
(21) Belous, A. G.; Novitsukaya, G. N.; Polyanetkaya, S. V.; Gornikov, Y. I. *Izv. Akad. Nauk SSSR, Neorg. Mater.* **1987**, *23*, 470.
(22) Kawai, H.; Kuwano, J. *J. Electrochem. Soc.* **1994**, *141*, L78–L79.
(23) Stramare, S.; Thangadurai, V.; Weppner, W. *Chem. Mater.* **2003**, *15*, 3974–3990.
(24) Ramya, C. S.; Selvasekarapandian, S.; Hirankumar, G.; Savitha, T.; Angelo, P. C. *J. Non-Cryst. Solids* **2008**, *354*, 1494–1502.
(25) Li, X.; Hsu, S. L. *J. Polym. Sci., Polym. Phys.* **1984**, *22*, 1331–1342.
(26) Hodge, I. M.; Ingram, M. D.; West, A. R. *J. Electroanal. Chem. Interfacial Electrochem.* **1976**, *74*, 125–143.
(27) Roman, H. E.; Bunde, A.; Dieterich, W. *Phys. Rev. B* **1986**, *34*, 3439–3445.
(28) Croce, F.; Persi, L.; Ronci, F.; Scrosati, B. *Solid State Ionics* **2000**, *135*, 47–52.
(29) Ji, K.; Moon, H.; Kim, J.; Park, J. *J. Power Sources* **2003**, *117*, 124–130.
(30) Chung, S. H.; Wang, Y.; Persi, L.; Croce, F.; Greenbaum, S. G.; Scrosati, B.; Plichta, E. *J. Power Sources* **2001**, *97–98*, 644–648.
(31) Xi, J.; Tang, X. *Chem. Phys. Lett.* **2004**, *393*, 271–276.
(32) Kuo, C. W.; Huang, C. W.; Chen, B. K.; Li, W. B.; Chen, P. R.; Ho, T. H.; Tseng, C. G.; Wu, T. Y. *Int. J. Electrochem. Sci.* **2013**, *8*, 3834–3850.
(33) Croce, F.; Focarete, M. F.; Hassoun, J.; Meschinia, I.; Scrosati, B. *Energy Environ. Sci.* **2011**, *4*, 921–927.
(34) Chiang, C. Y.; Reddy, M. J.; Chu, P. P. *Solid State Ionics* **2004**, *175*, 631–635.
(35) Chu, P. P.; Reddy, M. J.; Kao, H. M. *Solid State Ionics* **2003**, *156*, 141–153.
(36) Wagemaker, M.; Kearley, G. J.; Well, A. A.; Mutka, H.; Mulder, F. M. *J. Am. Chem. Soc.* **2003**, *125*, 840–848.

DOI: 10.1021/acs.nanolett.5b00600
Nano Lett. 2015, 15, 2740–2745

(37) Wieczorek, W.; Florjanczyk, Z.; Stevens, J. R. *Electrochim. Acta* **1995**, *40*, 2251−2258.
(38) Wang, Z. X.; Huang, X. J.; Chen, L. Q. *Electrochem. Solid-State Lett.* **2003**, *6*, E40−E44.

DOI: 10.1021/acs.nanolett.5b00600
Nano Lett. 2015, 15, 2740−2745